



HAL
open science

Looking into the dynamics of molecular crystals of ibuprofen and terephthalic acid using ^{17}O and ^2H NMR analyses

Chia-hsin Chen, Ieva Goldberga, Philippe Gaveau, Sébastien Mittelette, Jessica Špačková, Chuck Mullen, Ivan Petit, Thomas-Xavier Métro, Bruno Alonso, Christel Gervais, et al.

► To cite this version:

Chia-hsin Chen, Ieva Goldberga, Philippe Gaveau, Sébastien Mittelette, Jessica Špačková, et al.. Looking into the dynamics of molecular crystals of ibuprofen and terephthalic acid using ^{17}O and ^2H NMR analyses. *Magnetic Resonance in Chemistry*, 2021, 59, pp.975. 10.1002/mrc.5141 . hal-03205685

HAL Id: hal-03205685

<https://hal.science/hal-03205685>

Submitted on 22 Apr 2021

HAL is a multi-disciplinary open access archive for the deposit and dissemination of scientific research documents, whether they are published or not. The documents may come from teaching and research institutions in France or abroad, or from public or private research centers.

L'archive ouverte pluridisciplinaire **HAL**, est destinée au dépôt et à la diffusion de documents scientifiques de niveau recherche, publiés ou non, émanant des établissements d'enseignement et de recherche français ou étrangers, des laboratoires publics ou privés.



Distributed under a Creative Commons Attribution - NonCommercial - NoDerivatives 4.0 International License

Looking into the dynamics of molecular crystals of ibuprofen and terephthalic acid using ^{17}O and ^2H NMR analyses

Chia-Hsin Chen,^{1,†} Ieva Goldberga,^{1,†} Philippe Gaveau,¹
Sébastien Mittlette,¹ Jessica Špačková,¹ Chuck Mullen,² Ivan Petit,³
Thomas-Xavier Métro,⁴ Bruno Alonso,¹ Christel Gervais,³ Danielle Laurencin^{1,*}

1 ICGM, Univ Montpellier, CNRS, ENSCM, Montpellier, France

2 PhoenixNMR, 510 E. 5th Street Loveland CO, 80537, USA

3 Laboratoire de Chimie de la Matière Condensée de Paris (LCMCP), UMR 7574, Sorbonne Université, CNRS, 75005 Paris, France

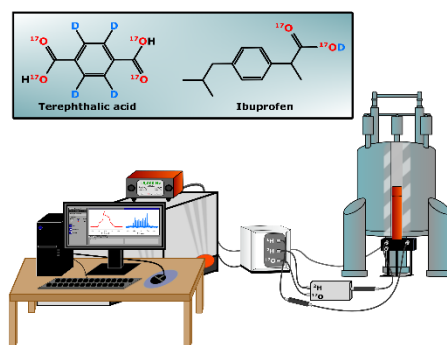
4 IBMM, Univ Montpellier, CNRS, ENSCM, Montpellier, France

[†] CH C and IG contributed equally to this work

* To whom correspondence should be addressed : danielle.laurencin@umontpellier.fr

Abstract

Oxygen-17 and deuterium are two quadrupolar nuclei that are of interest for studying the structure and dynamics of materials by solid state NMR. Here, ^{17}O and ^2H NMR analyses of crystalline ibuprofen and terephthalic acid are reported. First, improved ^{17}O -labelling protocols of these molecules are described using mechanochemistry. Then, dynamics occurring around the carboxylic groups of ibuprofen are studied considering variable-temperature ^{17}O and ^2H NMR data, as well as computational modelling (including molecular dynamics simulations). More specifically, motions related to the concerted double proton jump and the 180° flip of the H-bonded $(-\text{COOH})_2$ unit in the crystal structure were looked into, and it was found that the merging of the C=O and C-OH ^{17}O resonances at high temperatures cannot be explained by the sole presence of one of these motions. Lastly, preliminary experiments were performed with a ^2H - ^{17}O diplexer connected to the probe. Such configurations can allow, among others, ^2H and ^{17}O NMR spectra to be recorded at different temperatures without needing to tune or to change probe configurations. Overall, this work offers a few leads which could be of use in future studies of other materials using ^{17}O and ^2H NMR.



Introduction

The potential of solid-state NMR techniques for helping study the structure and reactivity of complex (bio)molecular and materials systems has significantly increased in recent years, thanks to numerous developments made in terms of instrumentation (e.g., ultra-high magnetic fields, ultra-fast magic angle spinning – MAS – probes),¹⁻³ pulse-sequence developments (e. g. ¹H-detected sequences, ultra-wide line and broadband acquisition methods),^{2, 4-8} more efficient and/or selective isotopic enrichment approaches,⁹⁻¹² as well as Dynamic Nuclear Polarization (DNP).¹³⁻¹⁴ Studies on challenging quadrupolar nuclei of low receptivity are increasingly being reported, including for some of the most « exotic » ones,¹⁵⁻¹⁶ like ⁴³Ca, ⁶¹Ni, ⁸⁷Sr and ⁹⁰Zr, just to name a few. Moreover, investigations aiming at understanding the dynamics occurring at different timescales within (bio)molecular and materials systems are seen as highly important, not only because of the impact they can have on the NMR spectra and their acquisition conditions, but also and more importantly because of the insight they can provide on the properties of a given (bio)molecule or material.¹⁷⁻²¹

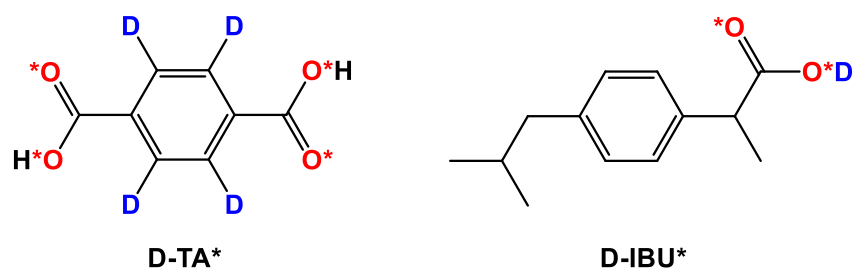
When it comes to studying dynamics in materials involving small organic molecules, ²H and ¹⁷O are both attractive quadrupolar nuclei.²²⁻²⁹ This is notably true in crystals composed of molecules with carboxylic acid groups associated as dimers. Indeed, the dynamics of protons « hopping » between the H-bonded C=O and C-OH groups have been the object of much research, including using ²H and ¹⁷O magnetic resonance techniques.^{24, 30-32} Among recent ²H studies, Schmidt and Sebastiani's work showed by *ab initio* calculations that the ²H quadrupolar parameters in strongly H-bonded systems could not be directly transposed into structural data such as bond lengths, due to the importance of non-linear effects and collective motions.³² Regarding ¹⁷O, Wu and co-workers' investigations are worth highlighting: they demonstrated by using variable temperature ¹⁷O NMR analyses that it is possible to study the concerted double-proton jumping, and estimate the energy asymmetry between the two H-bonded tautomers experimentally.²⁴ More generally speaking, when looking at the available literature, it appears that the information arising from ²H and ¹⁷O NMR analyses can potentially provide complementary information on the dynamic processes taking place within carboxylic acid dimers.

Considering the above context, the purpose of this article is to expand the possibilities for studying dynamics within molecular crystals by ²H and ¹⁷O NMR. Our studies were performed on two molecules: terephthalic acid and ibuprofen. Because of the very low natural abundance of both isotopes (Table 1), analyses were performed on enriched samples. First, improved ¹⁷O-labelling protocols based

on mechanochemistry are described for both molecules.³³ They were used to produce two doubly labelled compounds (enriched in ^2H and ^{17}O), referred to as **D-TA*** and **D-IBU***, which were isolated as molecular crystals (Scheme 1). Second, a variable temperature ^{17}O MAS NMR study of **D-IBU*** is presented. The ^{17}O NMR spectra are discussed using complementary computational modelling studies, including molecular dynamics simulations and *ab initio* calculations of NMR parameters. Lastly, preliminary NMR investigations involving a ^2H - ^{17}O diplexer connected to the NMR probe are presented. This system was used in the case of **D-TA***, enabling some of the ^2H and ^{17}O NMR experiments to be performed at different temperatures in a back-to-back fashion with no need to retune the probe. This configuration is not standard considering the very similar Larmor frequencies of both nuclei (Table 1). Overall, the results presented in this manuscript will be of interest for future investigations of structure and dynamics using ^{17}O and/or ^2H NMR.

Table 1. Nuclear spin properties of ^1H , ^2H and ^{17}O

	^1H	^2H	^{17}O
Spin	1/2	1	5/2
Natural abundance	99.98%	0.015%	0.037%
Larmor frequency ν_0 (MHz) at 14.1 T	600.1	92.1	81.4
Quadrupole moment Q ($\times 10^{-30} \text{ m}^2$)³⁴	/	2.86	-25.58



Scheme 1. Structures of the doubly-labelled ^{17}O and ^2H molecules: terephthalic acid (left) and ibuprofen (right). ^{17}O labelling was achieved using mechanochemistry.³⁵

Experimental section

Isotopic labelling procedures for terephthalic acid and ibuprofen

The following reagents were used as received: ibuprofen ($C_{13}H_{18}O_2$, Sigma Aldrich, $\geq 98\%$ purity, racemic form, noted here IBU), terephthalic acid ($C_8H_6O_4$, Janssen Chemicals, 98% purity, noted here TA), deuterated terephthalic acid ($C_8D_4H_2O_4$, with full deuteration on the aromatic cycle, 98% purity, Cambridge Isotope Laboratories, noted here D-TA) 1,1'-carbonyldiimidazole ($C_7H_6N_4O$, TCI, $>97\%$ purity, noted here CDI).

^{18}O -labelled water was purchased from Eurisotop (isotopic composition indicated in the certificate of analysis: 97.1% ^{18}O , 1.1% ^{17}O , 1.8% ^{16}O) or CortecNet (isotopic composition indicated in the certificate of analysis: 99.3% ^{18}O , 0.2% ^{17}O , 0.5% ^{16}O), and used for the optimisation of the enrichment protocols of terephthalic acid and ibuprofen, respectively, as detailed below.

^{17}O -labelled water was purchased from CortecNet. The isotopic composition indicated in the certificate of analysis was 8.6% ^{18}O , 90.4% ^{17}O , 1.0% ^{16}O for the $\sim 90\%$ ^{17}O -enriched H_2O , and 43% ^{18}O , 41% ^{17}O , 16% ^{16}O for the $\sim 40\%$ ^{17}O H_2O .

D_2O ($> 99.96\%$, CAS 7789-20-0) was purchased from Sigma-Aldrich.

Reagent grade solvents were used in all purification protocols.

^{17}O -enrichment of terephthalic acid and deuterated terephthalic acid by mechanochemistry

The enrichment procedure was first optimised using ^{18}O -enriched water, due to its lower cost compared to ^{17}O -enriched water. Terephthalic acid (50 mg, 0.30 mmol, 1.0 eq) and CDI (107 mg, 0.66 mmol, 2.2 eq) were introduced in a stainless-steel grinding jar (10 mL inner volume) with two stainless steel balls (10 mm diameter). The jar was closed and subjected to grinding for 60 minutes in the MM400 mixer mill operating at 25 Hz. ^{18}O -labelled water (16 μL , 0.88 mmol, ~ 3 eq) was then introduced in the jar, and the mixture was subjected to further grinding for 60 minutes at 25 Hz. To help recover the product, non-labelled water (1 mL) was introduced in the jar, and the medium was subjected to grinding for 2 minutes at 25 Hz. Then, it was transferred to an Erlenmeyer flask (together with 2x1 mL of non-labelled water, used here to rinse the grinding jar). The medium was acidified to pH ~ 1 by adding a few drops of concentrated HCl (6 mol.L $^{-1}$ aqueous solution, ~ 15 drops). The white precipitate was immediately filtered on a glass frit, washed with 4x0.5 mL of a 1 mol.L $^{-1}$ aqueous solution of HCl, and

then with 0.5 mL of ultrapure water. The recovered solid was dried overnight under vacuum. Average yield ($n = 3$, n representing the number of independent labelling experiments performed): 43 mg, 86 %. Average ^{18}O -enrichment level per oxygen, as determined by MS ($n = 3$) = $46 \pm 1\%$.

For the preparation of the ^{17}O - and ^2H -enriched phase (noted **D-TA***), D_4 -terephthalic acid was used as a precursor, and the ^{17}O -labelling step was performed following the optimised ^{18}O -enrichment protocol described above using $\sim 40\%$ ^{17}O -labelled water for the hydrolysis step instead (yield: 42 mg; average ^{17}O -enrichment level per oxygen, as determined by MS = $20 \pm 1\%$). The ^1H and ^{13}C solution NMR spectra, ESI-MS spectrum and XRD powder pattern of **D-TA*** are shown in supporting information (Figures S1 to S3).

^{17}O -enrichment of ibuprofen by mechanochemistry

The enrichment procedure was first optimised using ^{18}O -enriched water, due to its lower cost compared to ^{17}O -enriched water. Ibuprofen (120 mg, 0.58 mmol, 1.0 eq) and CDI (103 mg, 0.64 mmol, 1.1 eq) were introduced into a Retsch MM400 stainless steel grinding jar (10 mL inner volume) containing two stainless steel balls (10 mm diameter). The jar was closed and subjected to grinding for 30 minutes in the MM400 mixer mill operating at 25 Hz. ^{18}O -labelled water (99.3%, 16 μL , 0.87 mmol, 1.5 eq) was then added into the jar, and the mixture was subjected to further grinding for 30 minutes at 25 Hz. To help recover the product, non-labelled water (2 mL) was added into the jar, and the content was subjected to grinding for 2 minutes at 25 Hz. Then, the medium was transferred to a beaker (together with a sufficient amount of non-labelled water (8 mL) used here to rinse the jar). The medium was then acidified to $\text{pH} \sim 1$ with an aqueous solution of HCl (6 $\text{mol}\cdot\text{L}^{-1}$, 18 drops). The white precipitate was filtered on a glass frit, and 2x5 mL of non-labelled water was used to help recover the rest of the product from the beaker. The product was washed with a 1 $\text{mol}\cdot\text{L}^{-1}$ aqueous solution of HCl and ultrapure water (3x1 mL of each), and then dried under vacuum. Average synthetic yield ($n=3$): 89 mg, 75%. Average ^{18}O -enrichment level per oxygen, as determined by MS ($n=3$): $45 \pm 2\%$.

For the preparation of the ^{17}O -enriched phase (noted **IBU***), the ^{17}O -labelling step was first performed following the optimised ^{18}O -enrichment protocol described above, but using 90.4% ^{17}O -labelled water (16 μL , 1.5 eq.) for the hydrolysis step. Synthetic yield: 96 mg, 79%. Average ^{17}O -enrichment level per oxygen, as determined by MS = $36 \pm 2\%$ (average of 5 measurements). The ^1H

and ^{13}C solution NMR spectra, ESI-MS spectrum, and XRD powder pattern of IBU* are shown in supporting information (Figures S4 to S6).

^2H -enrichment of ^{17}O -labelled ibuprofen

The deuteration step was performed by mixing 59.4 mg of ^{17}O -labelled ibuprofen (IBU*) with 0.5 mL of D_2O (~ 95 eq) in a 1.0 mL Eppendorf tube. The sample was sonicated for 1 minute to ensure good mixing of the reagents. The mixture was then left for 3 days on a laboratory rocker shaker (Stuart SSL4 – Rocker), with 70 oscillations per minute at room temperature. The mixture was spun down at 20 000 rpm for 15 minutes, and the excess water was discarded. The sample was then freeze-dried under vacuum for 6 hours to remove the rest of the water. Synthetic yield: 56.4 mg, 95%. The IR and XRD powder patterns of the doubly-labelled product **D-IBU*** can be found in supporting information (Figures S4 and S8). A similar ^2H -labelling protocol was also applied to non-labelled ibuprofen, on which complementary ^2H MAS NMR experiments were performed.

General characterisation protocols of the enriched compounds

Infrared (IR) spectra were recorded on a Perkin Elmer Spectrum 2 FT-IR instrument. The attenuated total reflectance (ATR) measurement mode was used (diamond crystal), and measurements were performed in the $400\text{-}4000\text{ cm}^{-1}$ range.

Powder XRD analyses were carried out on an X'Pert MPD diffractometer using $\text{Cu K}\alpha_1$ radiation ($\lambda = 1.5406\text{ \AA}$) with the operation voltage and current maintained at 40 kV and 25 mA, respectively. Diffractograms were recorded between 5° and 50° (or 60°) in 2θ , with a step size of 0.017° , and a time per step of 20 to 40 s.

Mass spectrometry (MS) analyses were performed on a Waters Synapt G2-S apparatus, using electrospray ionisation in negative mode in a range of 50-1500 Da. Capillary and cone voltages were set to 3000 V and 30 V, respectively. The source temperature was $100\text{ }^\circ\text{C}$ and the desolvation temperature was set to $250\text{ }^\circ\text{C}$. Data were processed by MassLynxV4.1 software. For each product, a solution was prepared (in ethanol or DMSO, depending on the solubility), which were analysed five-times by ESI-MS.

^1H and ^{13}C solution NMR spectra were recorded on an Avance III Bruker 600 MHz spectrometer equipped with a TCI Prodigy cryoprobe, using $\text{DMSO-}d_6$ as a solvent. Chemical shifts were referenced to the residual solvent peaks at 2.50 ppm (^1H NMR spectra) and 39.52 ppm (^{13}C NMR spectra).

The melting points of ibuprofen (IBU) and its enriched counterparts (IBU* and D-IBU*) were measured on a Büchi B-540 Melting Point Apparatus. Samples were heated up to 70°C, and then with a ramp of 1 °C/min up to 80 °C. All measurements were done in triplicate (n = 3) and are reported in Table S1 (supporting information). The ^2H and ^{17}O NMR spectra of melted D-IBU* are shown in Figure S9.

Solid-state NMR experiments

Solid-state NMR experiments were performed on a Varian VNMRs 600 MHz (14.1 T) spectrometer, using, in the vast majority of cases, a PhoenixNMR HXY probe equipped with a 3.2 mm probe head. The PhoenixNMR probe was tuned to ^1H (599.82 MHz), ^2H (92.07 MHz) and ^{17}O (81.33 MHz), using a ^2H - ^{17}O diplexer. Conversion from multiple to single port tuning required a “special” tuning plug-in and diplexer built specifically for ^2H and ^{17}O . RF for ^2H and ^{17}O from the NMR console goes through a PhoenixNMR diplexer that provides >100dBc isolation, and then into the probe on a single channel. The PhoenixNMR probe is adapted to provide an over-coupled double resonant structure for the ^2H and ^{17}O frequencies, which in conjunction with the diplexer can allow the observation of one channel while irradiating on the other. Spectra were recorded under static or MAS conditions, with spinning speeds ranging from 5 to 18 kHz, depending on the sample. In the case of the ^2H -enriched ibuprofen (not labelled in ^{17}O), complementary ^2H MAS NMR experiments were performed on a Varian T3 HX probe, tuned to ^2H and ^1H , and spinning at 5 kHz.

^{17}O NMR experiments were recorded using DFS (double frequency sweep) pulse sequence with a rotor-synchronised echo of one rotor period. The parameters were as follows: DFS pulse of 500 μs ($v_{\text{RF}}(^{17}\text{O}) \sim 7.4$ kHz), with a sweep between 70 and 200 kHz, followed by a ^{17}O excitation pulse of 2 μs , echo delay of 55.55 μs , and a π -pulse of 4 μs . All experiments were performed with a MAS frequency of 18 kHz, recycle delay of 0.5 s, and the number of transients acquired was 2400 for D-TA* and 4000 for D-IBU*. ^{17}O MAS NMR chemical shifts were referenced to D_2O at -2.7 ppm (which corresponds to tap-water at 0 ppm). The ^{17}O nutation experiment was also recorded using D_2O at room temperature (with a natural abundance of ^{17}O).

The ^2H NMR experiments performed on the PhoenixNMR probe were carried out using a solid echo pulse sequence with a $\pi/2$ pulse length of 3.7 μs . ^2H MAS NMR experiments on D-TA* were performed with a MAS frequency of 5 kHz and rotor-synchronised echo delay of one rotor period (200 μs), and spectra were acquired using 14000 transients and recycle delay of 0.5 s. Static experiments were performed on D-IBU*, using an echo delay of 30 μs , and acquiring 122500 transients with a recycle delay of 0.5 s. ^2H chemical shifts were referenced to pure D_2O at 4.6 ppm. The ^2H nutation experiment was also recorded using D_2O at room temperature.

The ^1H nutation experiment was recorded using adamantane at room temperature with a MAS frequency of 10 kHz.

Variable-temperature studies were carried out under static or magic-angle spinning conditions (spinning at 5 or 18 kHz). In each situation, the temperature was calibrated using $\text{Pb}(\text{NO}_3)_2$.³⁶ When working under MAS conditions, careful attention was paid to the setting of the magic angle using KBr (^{79}Br resonance). The accuracy of the magic-angle at each temperature of analysis could be verified on D-TA*, by the absence of symmetric splitting of the ^2H resonance and sidebands under magic angle spinning (see supporting information, Figure S10). If judged necessary, the magic-angle was carefully reset at the temperature of interest using KBr.

Computational details

The NMR chemical shift calculations were performed within the DFT formalism using the QUANTUM-ESPRESSO (QE)³⁷ software. The PBE generalised gradient approximation³⁸ was used and the valence electrons were described by norm-conserving pseudopotentials³⁹ in the Kleinman-Bylander form.⁴⁰ The wave functions were expanded on a plane wave basis set with kinetic energy cut-off of 80 Ry. The shielding tensor was computed using the Gauge Including Projector Augmented Wave (GIPAW)⁴¹ approach, which permits the reproduction of the results of a fully converged all-electron calculation. Absolute shielding tensors are obtained. The isotropic chemical shift δ_{iso} is defined as $\delta_{\text{iso}} = -[\sigma - \sigma^{\text{ref}}]$, where σ is the isotropic shielding and σ^{ref} is the isotropic shielding of the same nucleus in a reference system as previously described.¹¹ The principal components V_{xx} , V_{yy} , and V_{zz} of the electric field gradient (EFG) tensor are obtained by diagonalisation of the tensor. The quadrupolar interaction can then be characterised by the quadrupolar coupling constant C_Q and the asymmetry parameter η_Q ,

which are defined as: $C_Q = eQV_{zz}/h$ and $\eta_Q = (V_{yy} - V_{xx})/V_{zz}$. The experimental values of the quadrupole moments of ^{17}O ($Q = -25.58 \times 10^{-30} \text{ m}^2$) and ^2H ($Q = +2.86 \times 10^{-30} \text{ m}^2$)⁴² were used to calculate C_Q .

Two crystallographic structures of racemic ibuprofen (CCDC 1041383 and 128796) were tested as starting points. The geometry optimisation of all atomic positions (keeping cell parameters fixed to experimental values) was performed for both low- and high-energy tautomers using the VASP code⁴³ and a Monkhorst–Pack k-space grid size of $2 \times 3 \times 2$. NMR parameters were then calculated keeping the relaxed atomic positions.

For the evaluation of the rotational barrier energy of the H-bonded $(-\text{COOH})_2$ dimeric unit in ibuprofen, the crystalline structure # CCDC 128796 was used as a starting point (because the ibuprofen dimer is at the centre of the unit cell, thereby facilitating the application of a geometrical torsion). The dihedral angle $C_{\text{ar}}-C_{(\text{H})}-\text{C}-\text{O}$ was varied and constrained, while the geometry of the rest of the molecule was optimised, and the energy subsequently calculated.

AIMD (Ab-initio Molecular Dynamics) simulations were carried out with the CP2K code⁴⁴ consisting in the Born–Oppenheimer MD (BOMD) with PBE electronic representation, including the Grimme (D3) correction for dispersion,⁴⁵ GTH pseudopotentials,⁴⁶ combined plane-wave, and TZVP basis sets.⁴⁷ The BOMD was performed using the NVT ensemble. The Nose–Hoover thermostat was used to control the average temperature at 300 K. Trajectories were accumulated over ~ 20 ps with a time step of 0.5 fs. ^2H and ^{17}O NMR calculations were performed with QE every 400 steps, *i.e.*, every 200 fs.

Results

Improved ^{17}O -enrichment protocols and preparation of doubly-labelled molecules

Due to the very low natural abundance of ^{17}O and ^2H (Table 1), isotopic labelling is needed in order to be able to perform variable temperature solid-state NMR analyses in a reasonable time. While the deuteration of the carboxyl group can be easily achieved by exposure of the molecules to an excess of D_2O , the ^{17}O -labelling of the carboxylic oxygen atoms is not as straightforward, notably due to the high cost of ^{17}O -enriched water (1 mL of 90% ^{17}O -enriched water can cost up to ~ 2600 €). A previous study showed that terephthalic acid and ibuprofen could be enriched in ^{17}O using mechanochemistry in a cost-efficient and user-friendly way.¹¹ However, our enrichment levels only averaged to $\sim 3\text{-}8$ % per

carboxylic oxygen for these molecules, which is ~ 2.5 to 7 times less than the maximum enrichment we could have expected based on the reactions and precursors involved. Hence, as part of this work, we first re-optimised the ^{17}O -enrichment protocols for these two molecules.

The ^{17}O -labelling procedure we have developed involves two ball-milling steps, which are performed back-to-back and followed by IR spectroscopy:^{11, 48} an activation of the carboxylic function using 1,1'-carbonyldiimidazole (CDI), followed by the hydrolysis of the acyl-imidazole intermediate using ^{17}O -enriched water. If either of these steps is incomplete, the final enrichment level decreases. We retested the reaction conditions for TA and IBU using ^{18}O -enriched water (due to its lower cost compared to ^{17}O -enriched water), and found that longer milling times (30-60 minutes, instead of 5-10 minutes) were needed to ensure a better mixing of the reagents and full completion of activation and hydrolysis (see Figure S7 for illustrations in the case of IBU). We verified the reproducibility of the newly-optimised enrichment protocols and then used them for the ^{17}O -labelling of terephthalic acid and ibuprofen. In the case of terephthalic acid, the optimised ^{17}O -enrichment protocol was applied to a deuterated form of the molecule (D-TA, fully deuterated on the aromatic cycle), while for ibuprofen, it was applied to the non-labelled form of the molecule. The average ^{17}O -enrichment level per carboxylic oxygen achieved was ~ 20 % for D-TA* (when using ~ 40% ^{17}O -labelled water for the hydrolysis), and ~ 36% for IBU* (when using ~ 90% ^{17}O -labelled water for the hydrolysis). The mass spectra of the ^{17}O -labelled molecules can be found in supporting information, together with other analyses that demonstrate the purity and crystallinity of the isolated molecules (^1H NMR, ^{13}C NMR, and powder X-ray diffraction) (see Figures S1 to S6).

For ibuprofen, the ^{17}O -enriched compound was then re-suspended in the presence of an excess of D_2O in order to exchange the carboxylic O-H group by O-D and form the doubly-labelled compound D-IBU*. This reaction was followed by IR spectroscopy by looking at the O-H vibration modes' replacement by O-D ones (see Figure S8). It is worth noting that after completion of the reaction, the NMR rotor was immediately packed and stored under vacuum in the freezer to avoid any back-exchange of the carboxylic deuterium with atmospheric humidity.

Variable temperature ^{17}O MAS NMR of ibuprofen: experiments and computational modelling

The ^{17}O MAS NMR spectra of D-IBU* were recorded at 14.1 T, while regulating the temperature between 0 and + 60°C (Figure 1). The ^{17}O spectra show two second-order quadrupolar lineshapes at

0 °C, which correspond to the C=O and C-OH groups. These signals progressively merge as the temperature is increased, leading to a single resonance with a characteristic second-order quadrupolar lineshape at 60 °C. A similar observation had been made in our previous ^{17}O NMR study of non-deuterated ibuprofen.¹¹ Fits of the spectra recorded at 0 °C and 60 °C can be found in supporting information (Figure S11). The fitted parameters at 0 °C (i.e. $\delta_{\text{iso}} = 308 \pm 2$ ppm and $|C_Q| = 7.9 \pm 0.1$ MHz for the C=O, and with $\delta_{\text{iso}} = 179 \pm 2$ ppm and $|C_Q| = 7.3 \pm 0.1$ MHz for the C-OH) were in line with those reported previously for non-deuterated ibuprofen, and with results from GIPAW-DFT calculations on the crystal structure.¹¹ A tentative fit of the data recorded at 60 °C was also performed, resulting in intermediate δ_{iso} and $|C_Q|$ values ($\delta_{\text{iso}} = 244 \pm 2$ ppm and $|C_Q| = 7.6 \pm 0.1$ MHz).

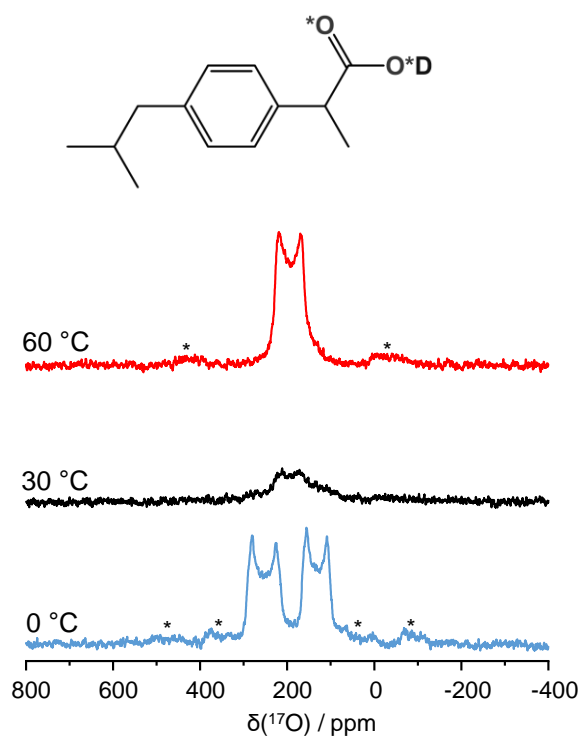
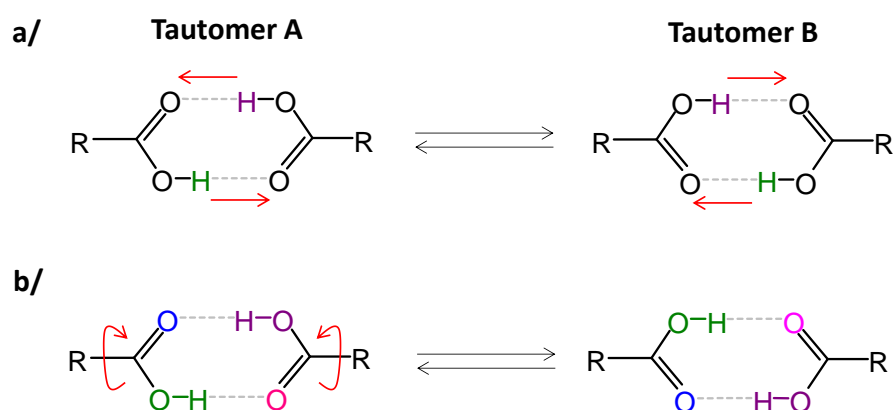


Figure 1. Variable-temperature ^{17}O MAS NMR spectra of D-IBU*. All ^{17}O NMR spectra shown here were recorded using the same acquisition conditions (including the same number of scans). The temperatures indicated correspond to the sample temperature inside the rotor at each spinning speed, as determined from calibrations using $\text{Pb}(\text{NO}_3)_2$. Tentative fits of the 0 °C and 60 °C spectra can be found in Supporting Information (Figure S11). « * » symbols correspond to spinning sidebands.

Although several polymorphs of racemic ibuprofen have been reported,⁴⁹ the most stable form was synthesized here, for which no polymorphic change is expected over the temperature range

investigated by NMR. The changes in ^{17}O solid-state NMR spectra around room temperature could, however, be due to (i) variations in the relative populations of the two tautomeric forms undergoing double proton jumps (Scheme 2a),²⁴ and/or (ii) 180° flips of the $(-\text{COOH})_2$ units (Scheme 2b),⁵⁰ the latter motion having been suggested to exist for ibuprofen by Geppi and co-workers.⁵¹ Both of these motions were further analysed, using additional computational simulations to help rationalise the observations made by ^{17}O NMR.



Scheme 2. Illustration of dynamics which can occur between H-bonded carboxylic acids, leading to interconversion between the two tautomeric forms: a/ concerted double proton jump and b/ concerted 180° flips of the H-bonded $(-\text{COOH})_2$ units.

First, the possible influence of concerted double proton jumps between the two tautomeric forms of ibuprofen on the ^{17}O MAS NMR data was looked into. Based on Wu and co-workers' recent work on a series of molecular crystals involving H-bonded carboxylic dimers, these motions can result in changes in ^{17}O NMR spectra with temperature, depending on the relative population of the tautomeric forms.²⁴ Such proton exchanges occur on the ps timescale and can participate in the averaging of ^{17}O NMR parameters between the two tautomeric forms. Here, a molecular dynamics simulation of racemic ibuprofen at 300 K was performed over a duration of 20 ps. This simulation brings evidence of the concerted double proton jumps, and shows the evolution of the calculated average ^{17}O NMR parameters of each oxygen (Figure 2), which appear to all progressively evolve towards averaged values.

Nevertheless, a full averaging of the ^{17}O NMR parameters could not be reached within the 20 ps timescale studied here.

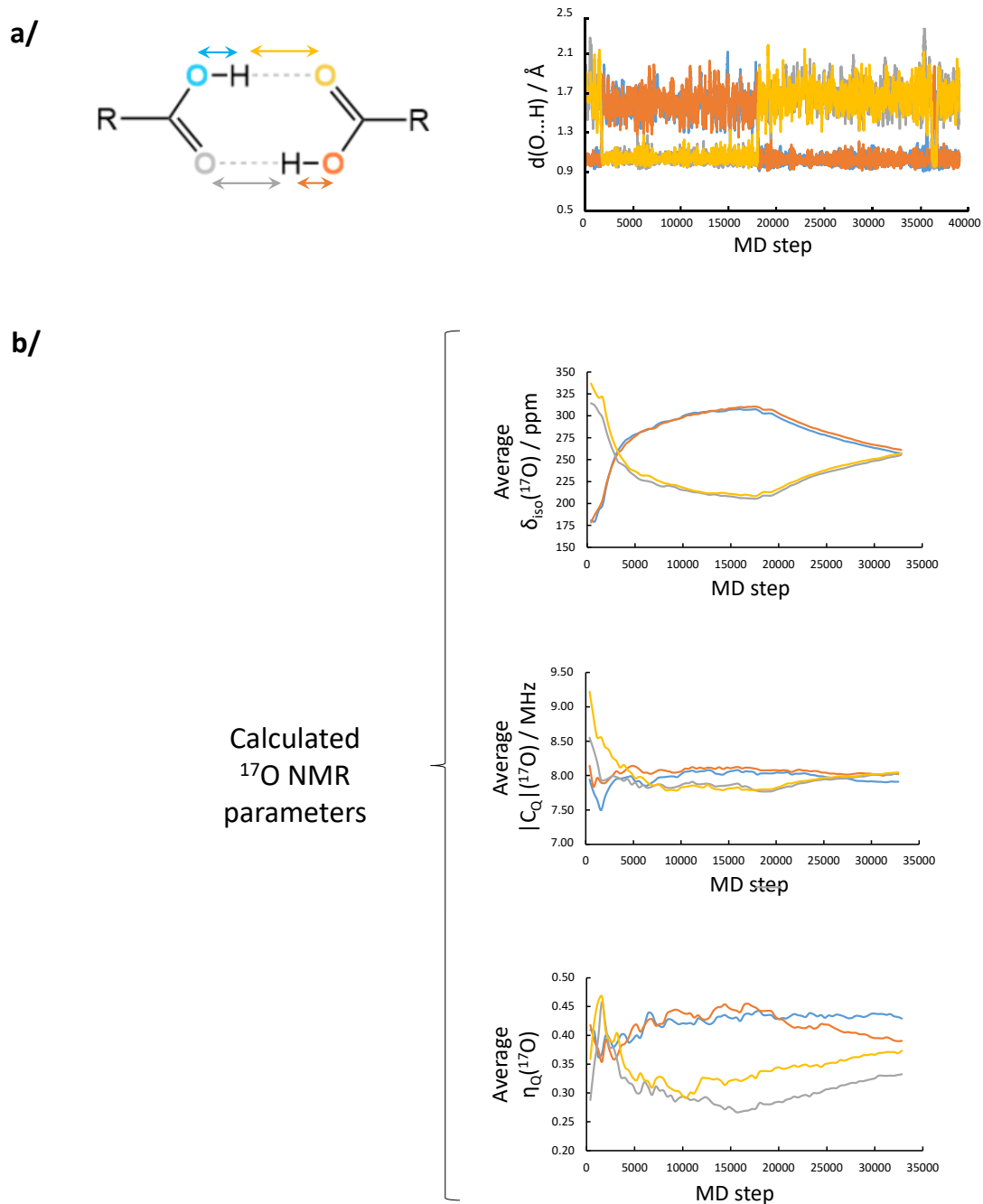


Figure 2. Molecular dynamics simulation of the structure of racemic ibuprofen, performed at 300 K, for a duration of 20 ps, with steps of 0.5 fs, with a focus on calculated ^{17}O NMR data.

a/ Evolution of the H \cdots O bond distances (in Å) in the dimer of the unit cell for which a concerted double ^1H jump was observed over the timescale of the calculation performed here (for the other dimer, no jump was observed); b/ Evolution of the DFT-calculated averaged ^{17}O NMR parameters for each oxygen site in this dimer (NMR parameters were calculated every 400 steps, *i. e.*, every 200 fs; and for each new point calculated along the MD, the new value was averaged with the previous ones).

For concerted double-proton jumps, the extent of averaging of the NMR parameters between both tautomers depends on the energy difference between the two forms and the analysis temperature.²⁴ In the case of racemic ibuprofen, Kolesov *et al.* reported an energy difference between both tautomers ~ 7.7 kJ/mol, based on Raman spectroscopy measurements.⁵² In our case, starting from the crystalline structure of racemic ibuprofen,⁵³ the energy difference between the tautomeric forms was calculated by DFT, yielding a value ~ 8.8 kJ/mol,⁵⁴ which is of the same order of magnitude as the experimental value of Kolesov. Using these energy differences and the DFT-calculated ^{17}O NMR parameters of each tautomer (Figure 3a), an approach similar to the one recently described by Wu and co-workers was then applied,²⁴ in order to see how the ^{17}O NMR parameters may vary with temperature (Figure 3b). The most significant variations were observed for the isotropic chemical shifts. Yet, based on these calculations, a change of less than 10 ppm would have been expected for the « C=O » and « C-OH »-like resonances over the temperature range studied here (green-shaded region, Figure 2b), regardless of the energy difference chosen (8.8 or 7.7 kJ/mol). Similar conclusions would also have been expected for deuterated ibuprofen, for which an intermediate energy difference ~ 6.7 kJ/mol between the two tautomeric forms has been derived from Raman spectroscopy analyses.⁵² Overall, this implies that no merging of the two ^{17}O signals as observed in Figure 1 would have been expected to arise from concerted double ^1H -jumps only, on the basis of the calculated ^{17}O NMR parameters of the two tautomers and their energy difference.

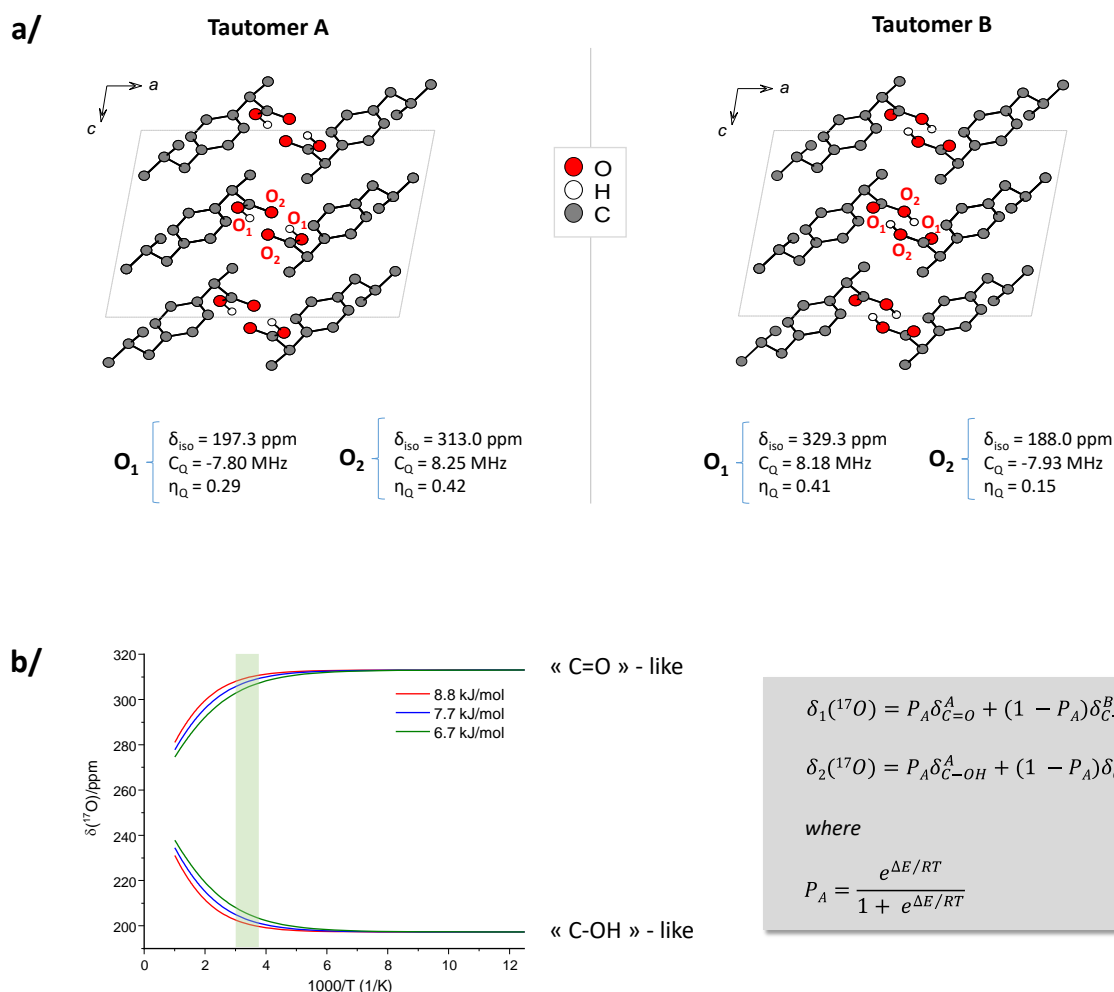


Figure 3. a/ Representation of the 2 tautomeric forms of ibuprofen and their DFT-calculated ^{17}O NMR parameters (for the $(-\text{COOH})_2$ dimer) (not all atoms in the unit cell are shown here for clarity); b/ Temperature dependency of the ^{17}O isotropic chemical shifts of the two tautomeric forms, for ΔE values of 8.8 kJ/mol (as calculated here by DFT for protonated ibuprofen) and of 7.7 and 6.7 kJ/mol (as determined experimentally by Raman for protonated and deuterated ibuprofen, respectively).⁵² The region shaded in green corresponds to the temperature range studied here by ^{17}O NMR (*i.e.* between 0 and 60 °C). The equations used for the plot are recalled in the grey-shaded box²⁴ (in which the DFT-calculated values of $\delta_{\text{C=O}}$ and $\delta_{\text{C-OH}}$ of the two tautomeric forms given in Figure 3a were used).

The motion related to a concerted rotation of the $(-\text{COOH})_2$ group was then looked into. As mentioned above, the presence of this 180° -flip had already been proposed in racemic ibuprofen on the basis of comprehensive ^1H and ^{13}C NMR analyses.⁵¹ Moreover, it is worth noting that the observations of the evolution of the variable-temperature ^{17}O MAS NMR spectra of ibuprofen recall those reported by Wu and co-workers for nicotinic acid, in which the 180° rotation of an H-bonded $-\text{COOH}$ unit was studied between ~ -20 and 100°C (although in the latter case, it is a single $-\text{COOH}$ moiety H-bonded to N which undergoes the 180° flip). Here, in contrast to the double proton jumps, the 180° -flip

motions in ibuprofen could not be made evident by molecular dynamics simulation due to the « short » timescale of our MD calculations. Nevertheless, the activation energy associated with this motion was evaluated by DFT, using an approach similar to the one proposed by Wu and co-workers for nicotinic acid.²² More specifically, starting from the published structure of racemic ibuprofen, the (-COOH)₂ dimeric fragment was rotated (keeping all other atomic positions constant), and the energy difference for each torsion angle was then calculated after the relaxation of all atomic positions (except for those defining the dihedral angle). Some of the calculated geometries are shown in Figure 4. In doing so, it was found that the energy barrier is ~ 75-100 kJ/mol (the value depending on the direction chosen for the rotation of the (-COOH)₂ unit). These values are very different from the one reported by Geppi on the basis of ¹H and ¹³C NMR analyses, which had estimated the barrier to ~ 13 kJ/mol. However, they are consistent with the energy barrier reported for (-COOH)₂ 180°-flips in other carboxylic dimers, for which values ranging from 50 to 85 kJ/mol have been reported.^{30, 55} Part of the difference with the value reported by Geppi may come from the fact that computationally, we are probing the rotation of the carboxylic group by « freezing » the rest of the structure, while in the experimental study, other motions are occurring within the crystal structure,^{51, 56-57} which may indirectly facilitate the rotation of the carboxylic dimer. Overall, although the experimental and computational data shown here does not yet achieve a complete picture of the (-COOH)₂ 180° flip and double proton exchange processes occurring in racemic ibuprofen, it nevertheless demonstrates the added value of performing high-resolution ¹⁷O NMR analyses and computational simulations to try to help understand these movements.

Torsion angle (°)	Relative energy (kJ/mol)
3.9	0.0
26.4	13.6
52.2	57.3
57.3	63.3
75.1	93.2
95.6	83.5
107.4	81.3
125.3	62.2
174.4	7.3
272.6	100.1
304.1	45.7
328.2	11.2

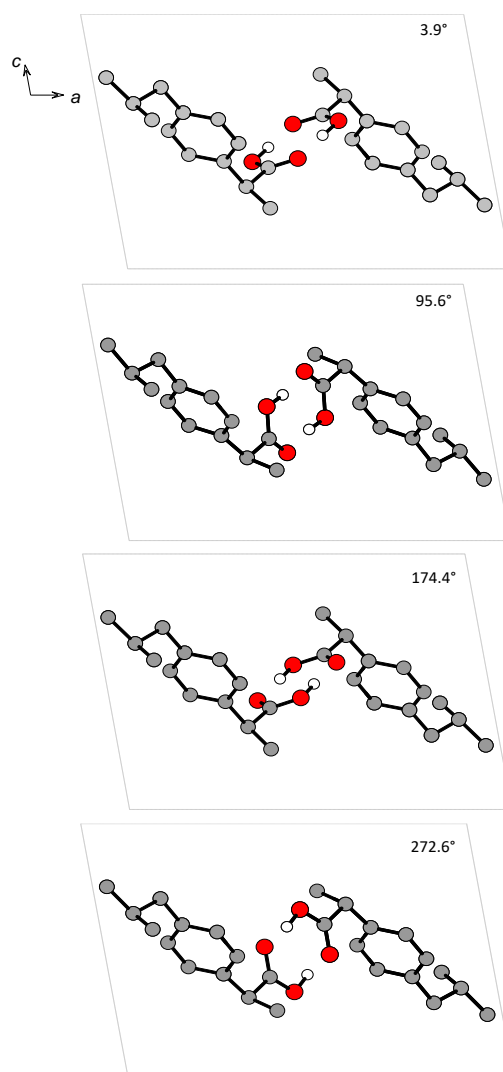


Figure 4. DFT-evaluation of the activation energy for the rotation of the $(-\text{COOH})_2$ dimeric unit in crystalline racemic ibuprofen (using the CCDC crystal structure # 128796). Illustrations of some of the torsion angles are shown on the right (with C, O, and H in grey, red and white, respectively; not all atoms in the unit cell are displayed here for clarity).

Variable temperature analyses using a ^1H - ^2H - ^{17}O tuning configuration

To complement the ^{17}O MAS NMR study of the H-bonded carboxylic groups dynamics in D-IBU*, ^2H NMR experiments were carried out. Here, the possibility of performing ^2H and ^{17}O NMR analyses in a back-to-back fashion was investigated, using a diplexer connected to the probe for ^1H - ^2H - ^{17}O tuning. Indeed, being able to analyse ^2H and ^{17}O local environments at any given temperature without changing

the NMR probe configuration can be attractive, especially to avoid hysteresis effects that can occur upon heating or cooling some crystalline phases.

A schematic illustration of the mode of connection of the diplexer to the NMR probe is shown in Figure 5a, with further details being provided experimental section. The nutations obtained upon calibration of RF pulses using D₂O for ²H and ¹⁷O, and adamantane for ¹H, are shown in Figure 5b. The loss in sensitivity of this triple resonance mode compared to the double resonance configuration was found to be reasonable (see supporting information, Figure S12).

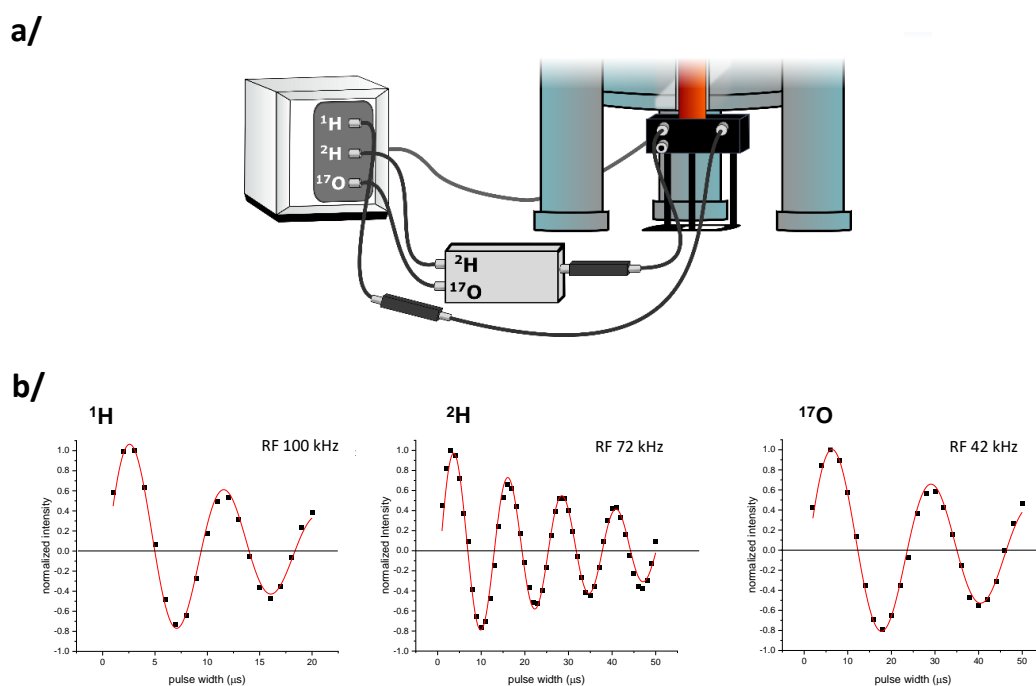


Figure 5. a/ Schematic representation of the connection mode of the diplexer to the NMR probe, and b/ nutations achieved on the ¹H, ²H and ¹⁷O channels in triple resonance mode. The 810°/90° intensity ratio determined here for ²H is 0.51.

This probe configuration was first tested on the doubly-labelled D-TA* phase due to its higher weight percentage in both ¹⁷O and ²H. The ²H and ¹⁷O MAS NMR spectra were recorded between -30 and +60 °C (Figure 6). No significant changes were observed in the ²H NMR. Although ²H relaxation measurements may have led to observable differences, these were not performed at this stage.

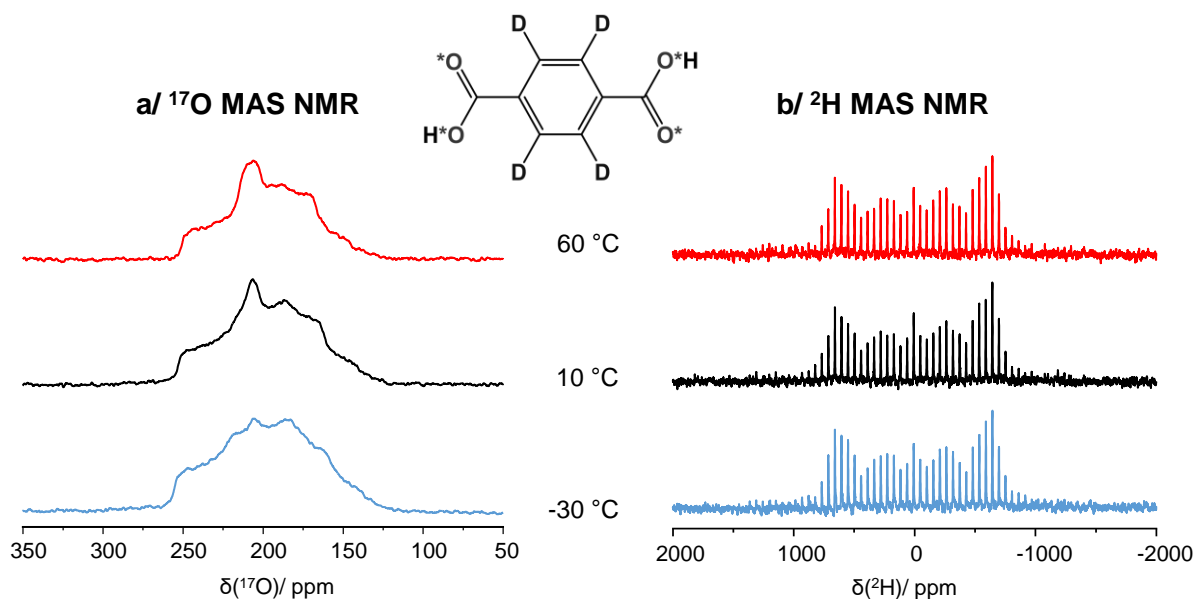


Figure 6. Variable temperature ^{17}O and ^2H NMR spectra of D-TA*, recorded under magic angle spinning conditions. The temperatures indicated correspond to the sample temperature inside the rotor, as determined from calibrations at different MAS speeds using $\text{Pb}(\text{NO}_3)_2$.

In the case of ^{17}O NMR, only subtle variations with temperature were observed. A tentative deconvolution of the spectra is shown in Figure S13 (supporting information), considering the presence of 2 resonances corresponding to « C=O » and « C-OH » like environments, in agreement with the previous ^{17}O NMR work reported for non-deuterated terephthalic acid.¹¹ Due to the overlap of both resonances, MQMAS experiments at each temperature of analysis (or variable-temperature analyses at a second magnetic field) would have been needed to confirm the fitted parameters. Nevertheless, the small variations observed for D-TA* over this temperature range may reflect effects of H-bonding tautomerism and/or polymorphic changes of terephthalic acid.⁵⁸⁻⁶⁴ Indeed, on the one hand, previous studies in the literature have shown that the H-bonded carboxylic protons of terephthalic acid are dynamically disordered at room temperature, undergoing concerted double-proton jumps (Scheme 2a).^{58, 63, 65} The fact that the free enthalpy difference between both tautomeric forms has been estimated experimentally to only ~ 2 kJ/mol⁶³ for terephthalic acid implies that small changes should be observable over the temperature range studied here (because this value is of the same order of magnitude as those reported for cinnamic acid and aspirin).²⁴

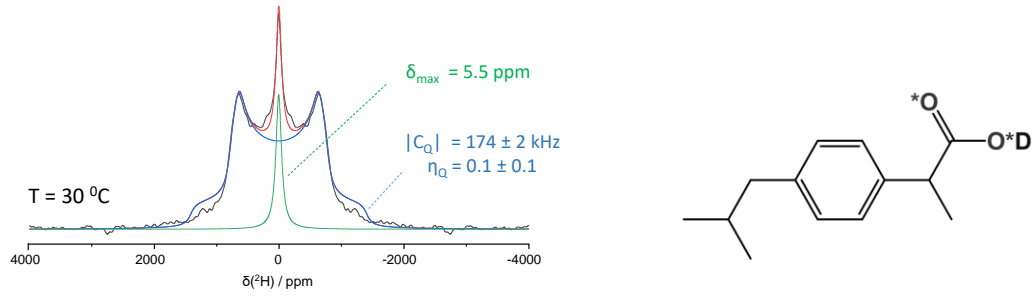
On the other hand, the variations in the ^{17}O MAS NMR spectra may also reflect the existence of several polymorphic forms of terephthalic acid. Out of the three polymorphs reported to date for this molecule, triclinic forms (I) and (II) have been the object of much attention.^{59-62, 64, 66} Both consist of

chains of terephthalic acid molecules, in which each molecule is hydrogen-bonded to 2 others through carboxylic acid dimer motifs. These chains are further assembled into 2D layers, which pack differently from one polymorph to the other. Moreover, when looking at the terephthalic acid motif itself, slightly different dihedral angles are found between the carboxylic function and the aromatic cycle when both polymorphs are compared.⁶⁴ Although both forms can be observed under ambient temperature and pressure, form (I) appears to be the least stable. Its transformation into form (II) has been studied both experimentally and computationally.^{59-60, 62} More specifically, this transformation was found to occur above 70 °C, to be sensitive to pressure, and to be caused by a « surface-mediated nucleation » type of process, triggered by the movement of the supramolecular chains of terephthalic acid at the surface of the crystallites.^{60, 62} In our case, given that D-TA* was obtained here as polymorph (I) (see Figure S1, supporting information), it is possible that the subtle modifications in the ¹⁷O NMR spectra upon heating are indicative of the onset of transformation into form (II), caused by the increase in temperature and possibly also pressure (due to the spinning). More specifically, ¹⁷O NMR may indicate that changes in the local environment of the carboxylic functions precede more significant movements of the supramolecular chains. Although the observations made in ¹⁷O NMR for D-TA* were not further investigated at this stage, they point to the interest of analysing molecular crystals by this technique, notably to help understand polymorphic transformations.

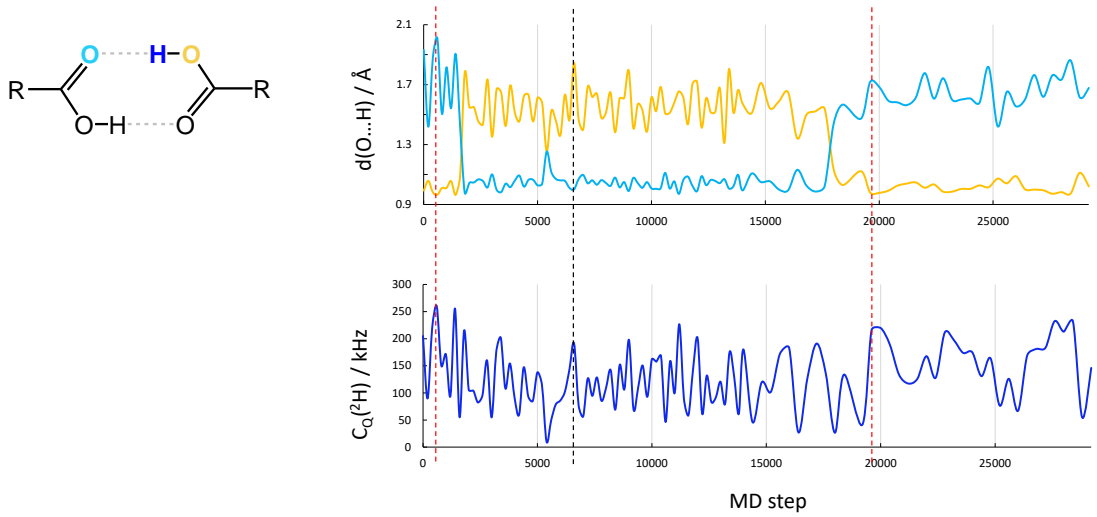
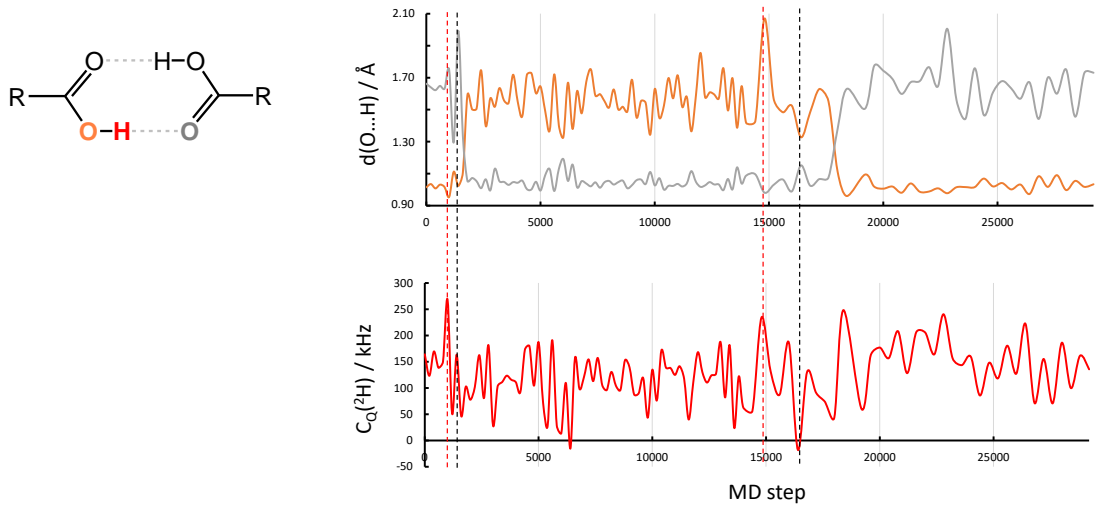
Using this ²H-¹⁷O probe configuration, preliminary ²H NMR studies were also performed in the case of D-IBU*. The static ²H NMR spectra revealed the presence of two main resonances (Figure 7a): one broad signal with a characteristic deuterium quadrupolar lineshape and a much sharper signal at the centre of the spectrum, the relative intensity of which was found to increase with temperature, under the measurement conditions used here (Figure S14, supporting information). The fitting of the broad ²H NMR signal at each temperature was performed, yielding similar quadrupolar parameters between 0 and 60 °C, with $|C_Q| \sim 170$ kHz and $\eta_Q \sim 0.1$ (Figure S14). These values are similar to those reported previously for supercooled and glassy states of deuterated ibuprofen,⁶⁷ as well as for other crystal structures of organic molecules involving H-bonded carboxylic dimers.⁶⁸ Hence, this ²H resonance is characteristic of (-COOD)₂ dimeric structures in crystalline D-IBU*, with the ²H NMR parameters being averaged between the two interconverting tautomeric forms of ibuprofen. The MD simulations and DFT calculations of ²H NMR parameters associated with these double proton jumps are provided in Figures 7b and 7c. In agreement with previous observations made by Sebastiani *et al.*³² for H-bonded carboxylic

acids, these calculations show that the « instantaneous » C_Q values tend to follow the evolution of the longer O...H distance (Figure 7b, dashed vertical lines).

a/



b/



c/

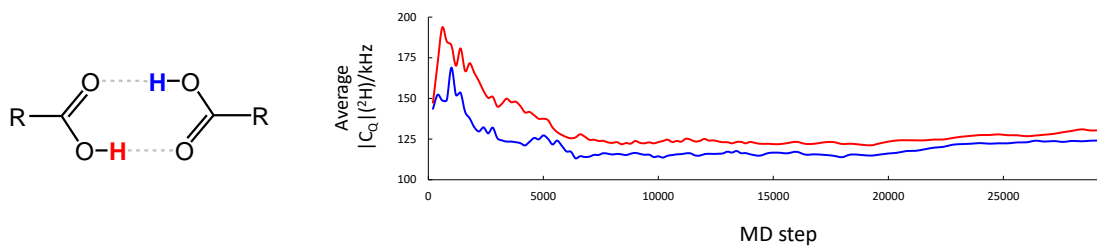


Figure 7. a/ Fit of the experimental static ^2H NMR spectrum of D-IBU* at 30°C, after symmetrisation of the ^2H lineshape (experimental spectrum in black, and its fit in red, considering two contributions, with in blue the H-bonded $-(\text{COOD})_2$ dimeric unit of D-IBU*, and in green the sharp mobile species. b/ Molecular dynamics simulation of the structure of racemic ibuprofen, performed at 300 K, with steps of 0.5 fs (shown here over a duration of ~ 15 ps), with a focus on calculated ^2H NMR data. Evolution of the H...O bond distances (in Å) in the dimer of the unit cell for which a concerted double proton jump was observed over the timescale of the calculation, and evolution of the « instantaneous » DFT-calculated ^2H quadrupolar coupling constant C_Q for this dimer (NMR parameters calculations were performed as a first approximation from the MD structures of protonated ibuprofen, every 200 steps, up to step # 14000, and then every 400 steps). c/ Evolution of the average calculated $|C_Q|$ values along with the MD timescale, showing that the ^2H $|C_Q|$ converges towards an average value.

The sharp central ^2H NMR resonance, on the other hand, is very weak at 0 °C, where it is centered at 5.2 ppm. At 60 °C, it becomes increasingly sharp and intense, and shifts to 9.4 ppm. Based on the observed chemical shifts and the ^2H NMR measurements also performed on melted D-IBU* (see Figures S9), this resonance appears to arise from different species: it is consistent with a small amount of residual liquid (mobile) water at 0 °C, and to the predominant presence of highly mobile ibuprofen at 60 °C (in a melt-like state, the melting temperature of ibuprofen being ~ 75 °C). It is worth noting that in comparison to previous variable-temperature ^2H NMR studies on supercooled and glassy ibuprofen,⁶⁷ the fully motionally-narrowed ^2H NMR signal is observed here at a higher temperature (80 °C in Figure S9, vs 36 °C in ref. ⁶⁷). Overall, it is clear that ^2H and ^{17}O NMR spectra provide complementary information regarding the dynamics occurring around the carboxylic groups in racemic ibuprofen. It can be hypothesized that the progressive increase in mobility within ibuprofen crystals with temperature (especially around the carboxylic function) allows some molecules to behave as in a melt-like state, which may favour dynamics like the 180° $(-\text{COOH})_2$ flip to occur with energy barriers lower than the ones calculated by DFT, thereby explaining the observations made by ^{17}O NMR. However, more extensive investigations would be needed to confirm this.

Conclusion

In this article, three different aspects related to the structural analysis of molecular crystals containing carboxylic functions have been looked into. First, improved ^{17}O labelling protocols based on mechanochemistry have been developed. This has allowed average enrichment levels exceeding 20% in ^{17}O per carboxylic oxygen to be reached for two key molecules: (i) ibuprofen, a non-steroidal anti-inflammatory drug which is seen as a « golden standard » for numerous investigations in pharmaceutical

sciences aiming at improving drug formulations, and (ii) terephthalic acid, which is one of the most commonly-used ligands for the design of metal-organic frameworks (MOFs). In the latter case, the ^{17}O labelling was performed here on a deuterated version of the terephthalic acid precursor (with deuteration on the aromatic ring), thereby leading to the formation of a doubly-labelled molecule, which would be of key interest for studying the structure and reactivity of a variety of MOFs, including the most complex ones. Such ligands should enable studying both the dynamics related to the 180° -flips of the aromatic ring (using ^2H NMR) and the binding properties to metal cations in a given system (using ^{17}O NMR).

Second, the experimental and computational study of ^{17}O and ^2H enriched ibuprofen has shed light on the interest in looking at both of these nuclei when studying the dynamics occurring around the carboxylic groups. Although further investigations would be needed to fully understand the experimental observations, this work nevertheless complements previous studies on racemic ibuprofen crystals involving ^1H and ^{13}C NMR, by underscoring the complexity of the molecular motions which take place around the carboxylic groups. More generally, this study shows how the NMR study of quadrupolar nuclei like ^{17}O and ^2H may provide new opportunities for investigating polymorphic transitions of ibuprofen,⁶⁹ as well as its confined or « supercooled » states.^{67, 70-71} Indeed, the polarity and H-bonding capability of carboxylic function implies that it is often key to interactions between molecules and with materials surfaces, meaning that direct insight into the local environment of the carboxylic atoms (among which oxygen) is important for detailed structure characterization purposes.

Lastly, we have presented some of the possibilities provided by combining ^2H - ^{17}O diplexers to NMR probes for studying by NMR the ^2H and ^{17}O nuclei at any given temperature, without having to change probe configurations. The RF-performance of the probe used along with the diplexer was shown to be suitable for such applications, as illustrated for both terephthalic acid and ibuprofen. While the experiments shown here were mainly performed in a back-to-back fashion, we will look into recording them using « double receiver » set-ups in future studies. Moreover, beyond these possibilities, the next step will consist of using such hardware configurations to perform multi-channel ^2H and ^{17}O correlation experiments. This pair of nuclear spins has not yet been studied due to the very similar Larmor frequencies of the two isotopes, but could offer new opportunities for helping understand further the structure of a variety of molecular and materials systems, considering that H and O are two atoms which are very often present. This is a point we will be looking into in the near future. Such instrumental developments will add to the ongoing effort to broaden the scope of heteronuclear correlations

accessible to NMR spectroscopists with spin pairs of similar Larmor frequencies (e.g., ^{13}C - ^{27}Al , $^{72-73}\text{ }^{13}\text{C}$ - ^{45}Sc , $^{73}\text{ }^{13}\text{C}$ - ^{81}Br ...⁷⁴).

Acknowledgements

This project has received funding from the European Research Council (ERC) under the European Union's Horizon 2020 research and innovation program (grant agreement No 772204; 2017 ERC-COG, MISOTOP project). NMR spectroscopic calculations were performed using HPC resources from GENCI-IDRIS (Grant 097535). Powder X-ray diffraction, mass spectrometry and solution NMR characterizations were performed with the support of the local Balard Plateforme d'Analyses et de Caractérisation (PAC Balard).

References

1. Gan, Z.; Hung, I.; Wang, X.; Paulino, J.; Wu, G.; Litvak, I. M.; Gor'kov, P. L.; Brey, W. W.; Lendi, P.; Schiano, J. L.; Bird, M. D.; Dixon, I. R.; Toth, J.; Boebinger, G. S.; Cross, T. A., NMR spectroscopy up to 35.2T using a series-connected hybrid magnet. *J. Magn. Reson.* **2017**, *284*, 125-136.
2. Ishii, Y.; Wickramasinghe, A.; Matsuda, I.; Endo, Y.; Ishii, Y.; Nishiyama, Y.; Nemoto, T.; Kamihara, T., Progress in proton-detected solid-state NMR (SSNMR): Super-fast 2D SSNMR collection for nano-mole-scale proteins. *J. Magn. Reson.* **2018**, *286*, 99-109.
3. Penzel, S.; Oss, A.; Org, M.-L.; Samoson, A.; Böckmann, A.; Ernst, M.; Meier, B. H., Spinning faster: protein NMR at MAS frequencies up to 126 kHz. *J. Biomol. NMR* **2019**, *73* (1), 19-29.
4. Wijesekara, A. V.; Venkatesh, A.; Lampkin, B. J.; VanVeller, B.; Lubach, J. W.; Nagapudi, K.; Hung, I.; Gor'kov, P. L.; Gan, Z.; Rossini, A. J., Fast Acquisition of Proton-Detected HETCOR Solid-State NMR Spectra of Quadrupolar Nuclei and Rapid Measurement of NH Bond Lengths by Frequency Selective HMQC and RESPDOR Pulse Sequences. *Chem. Eur. J.* **2020**, *26* (35), 7881-7888.
5. Zhang, R.; Mroue, K. H.; Ramamoorthy, A., Proton-Based Ultrafast Magic Angle Spinning Solid-State NMR Spectroscopy. *Acc. Chem. Res.* **2017**, *50* (4), 1105-1113.
6. Sanders, K. J.; Pell, A. J.; Wegner, S.; Grey, C. P.; Pintacuda, G., Broadband MAS NMR spectroscopy in the low-power limit. *Chem. Phys. Lett.* **2018**, *697*, 29-37.
7. Perras, F. A.; Venkatesh, A.; Hanrahan, M. P.; Goh, T. W.; Huang, W.; Rossini, A. J.; Pruski, M., Indirect detection of infinite-speed MAS solid-state NMR spectra. *J. Magn. Reson.* **2017**, *276*, 95-102.
8. O'Dell, L. A., Ultra-wideline Solid-State NMR: Developments and Applications of the WCPMG Experiment. In *Modern Magnetic Resonance*, Webb, G. A., Ed. Springer International Publishing: Cham, 2017; pp 1-22.
9. Gupta, S.; Tycko, R., Segmental isotopic labeling of HIV-1 capsid protein assemblies for solid state NMR. *J. Biomol. NMR* **2018**, *70* (2), 103-114.
10. Wong, V. W. C.; Reid, D. G.; Chow, W. Y.; Rajan, R.; Green, M.; Brooks, R. A.; Duer, M. J., Preparation of highly and generally enriched mammalian tissues for solid state NMR. *J. Biomol. NMR* **2015**, *63* (2), 119-123.
11. Métro, T.-X.; Gervais, C.; Martinez, A.; Bonhomme, C.; Laurencin, D., Unleashing the Potential of ¹⁷O NMR Spectroscopy Using Mechanochemistry. *Angew. Chem. Int. Ed. Engl.* **2017**, *129* (24), 6907-6911.
12. Hope, M. A.; Zhang, B.; Zhu, B.; Halat, D. M.; MacManus-Driscoll, J. L.; Grey, C. P., Revealing the Structure and Oxygen Transport at Interfaces in Complex Oxide Heterostructures via ¹⁷O NMR Spectroscopy. *Chem. Mater.* **2020**.
13. Lilly Thankamony, A. S.; Wittmann, J. J.; Kaushik, M.; Corzilius, B., Dynamic nuclear polarization for sensitivity enhancement in modern solid-state NMR. *Prog. Nucl. Magn. Reson. Spectrosc.* **2017**, *102-103*, 120-195.
14. Hooper, R. W.; Klein, B. A.; Michaelis, V. K., Dynamic Nuclear Polarization (DNP) 101: A New Era for Materials. *Chem. Mater.* **2020**, *32* (11), 4425-4430.
15. Leroy, C.; Bryce, D. L., Recent advances in solid-state nuclear magnetic resonance spectroscopy of exotic nuclei. *Prog. Nucl. Magn. Reson. Spectrosc.* **2018**, *109*, 160-199.
16. Bryce, D. L., New frontiers for solid-state NMR across the periodic table: a snapshot of modern techniques and instrumentation. *Dalton Trans.* **2019**, *48* (23), 8014-8020.
17. Matlahov, I.; van der Wel, P. C. A., Hidden motions and motion-induced invisibility: Dynamics-based spectral editing in solid-state NMR. *Methods* **2018**, *148*, 123-135.
18. Mandala, V. S.; Williams, J. K.; Hong, M., Structure and Dynamics of Membrane Proteins from Solid-State NMR. *Annu. Rev. Biophys.* **2018**, *47* (1), 201-222.
19. Milić, J. V.; Im, J.-H.; Kubicki, D. J.; Ummadisingu, A.; Seo, J.-Y.; Li, Y.; Ruiz-Preciado, M. A.; Dar, M. I.; Zakeeruddin, S. M.; Emsley, L.; Grätzel, M., Supramolecular Engineering for Formamidinium-Based Layered 2D Perovskite Solar Cells: Structural Complexity and Dynamics Revealed by Solid-State NMR Spectroscopy. *Adv. En. Mater.* **2019**, *9* (20), 1900284.

20. Dunstan, M. T.; Halat, D. M.; Tate, M. L.; Evans, I. R.; Grey, C. P., Variable-Temperature Multinuclear Solid-State NMR Study of Oxide Ion Dynamics in Fluorite-Type Bismuth Vanadate and Phosphate Solid Electrolytes. *Chem. Mater.* **2019**, *31* (5), 1704-1714.
21. Xiang, Y.-X.; Zheng, G.; Zhong, G.; Wang, D.; Fu, R.; Yang, Y., Toward understanding of ion dynamics in highly conductive lithium ion conductors: Some perspectives by solid state NMR techniques. *Solid State Ionics* **2018**, *318*, 19-26.
22. Lu, J.; Hung, I.; Brinkmann, A.; Gan, Z.; Kong, X.; Wu, G., Solid-State ¹⁷O NMR Reveals Hydrogen-Bonding Energetics: Not All Low-Barrier Hydrogen Bonds Are Strong. *Angew. Chem. Int. Ed. Engl.* **2017**, *56* (22), 6166-6170.
23. Wu, G., ¹⁷O NMR studies of organic and biological molecules in aqueous solution and in the solid state. *Prog. Nucl. Magn. Reson. Spectrosc.* **2019**, *114-115*, 135-191.
24. Wu, G.; Hung, I.; Gan, Z.; Terskikh, V.; Kong, X., Solid-State ¹⁷O NMR Study of Carboxylic Acid Dimers: Simultaneously Accessing Spectral Properties of Low- and High-Energy Tautomers. *J. Phys. Chem. A* **2019**, *123* (38), 8243-8253.
25. Catalano, J.; Murphy, A.; Yao, Y.; Zumbulyadis, N.; Centeno, S. A.; Dybowski, C., Molecular dynamics of palmitic acid and lead palmitate in cross-linked linseed oil films: Implications from deuterium magnetic resonance for lead soap formation in traditional oil paintings. *Solid State Nucl. Magn. Reson.* **2018**, *89*, 21-26.
26. Kolokolov, D. I.; Jobic, H.; Stepanov, A. G.; Guillerme, V.; Devic, T.; Serre, C.; Férey, G., Dynamics of Benzene Rings in MIL-53(Cr) and MIL-47(V) Frameworks Studied by 2H NMR Spectroscopy. *Angew. Chem. Int. Ed. Engl.* **2010**, *49* (28), 4791-4794.
27. Khudozhnikov, A. E.; Kolokolov, D. I.; Stepanov, A. G., Characterization of Fast Restricted Librations of Terephthalate Linkers in MOF UiO-66(Zr) by 2H NMR Spin–Lattice Relaxation Analysis. *J. Phys. Chem. C* **2018**, *122* (24), 12956-12962.
28. Jiang, X.; Duan, H.-B.; Jellen, M. J.; Chen, Y.; Chung, T. S.; Liang, Y.; Garcia-Garibay, M. A., Thermally Activated Transient Dipoles and Rotational Dynamics of Hydrogen-Bonded and Charge-Transferred Diazabicyclo [2.2.2]Octane Molecular Rotors. *J. Am. Chem. Soc.* **2019**, *141* (42), 16802-16809.
29. Dai, Y.; Terskikh, V.; Brinmkmann, A.; Wu, G., Solid-State 1H, 13C, and 17O NMR Characterization of the Two Uncommon Polymorphs of Curcumin. *Cryst. Growth Des.* **2020**, *20* (11), 7484-7491.
30. Scheubel, W.; Zimmermann, H.; Haeberlen, U., High-resolution 1H, 2H, and 13C solid-state NMR of dimethylmalonic acid. Detection of a new mode of hydrogen motion. *J. Magn. Reson.* **1988**, *80* (3), 401-416.
31. Kong, X.; Shan, M.; Terskikh, V.; Hung, I.; Gan, Z.; Wu, G., Solid-State ¹⁷O NMR of Pharmaceutical Compounds: Salicylic Acid and Aspirin. *J. Phys. Chem. B* **2013**, *117* (33), 9643-9654.
32. Schmidt, J.; Sebastiani, D., Anomalous temperature dependence of nuclear quadrupole interactions in strongly hydrogen-bonded systems from first principles. *J. Chem. Phys.* **2005**, *123* (7), 074501.
33. Friscic, T.; Mottillo, C.; Titi, H. M., Mechanochemistry for Synthesis. *Angew. Chem. Int. Ed. Engl.* **2019**, *59*, 1018-1029.
34. Pyykkö, P., Year-2017 nuclear quadrupole moments. *Mol. Phys.* **2018**, *116* (10), 1328-1338.
35. The ¹⁷O-labelling procedure leads to the predominant labelling of one oxygen per carboxylic group, but with both O atoms having the same probability to be enriched (which is why they are both highlighted in red).
36. Bielecki, A.; Burum, D. P., Temperature Dependence of ²⁰⁷Pb MAS Spectra of Solid Lead Nitrate. An Accurate, Sensitive Thermometer for Variable-Temperature MAS. *J. Magn. Reson., Ser. A* **1995**, *116* (2), 215-220.
37. Giannozzi, P.; Baroni, S.; Bonini, N.; Calandra, M.; Car, R.; Cavazzoni, C.; Ceresoli, D.; Chiarotti, G. L.; Cococcioni, M.; Dabo, I.; Dal Corso, A.; de Gironcoli, S.; Fabris, S.; Fratesi, G.; Gebauer, R.; Gerstmann, U.; Gougoussis, C.; Kokalj, A.; Lazzeri, M.; Martin-Samos, L.; Marzari, N.; Mauri, F.; Mazzarello, R.; Paolini, S.; Pasquarello, A.; Paulatto, L.; Sbraccia, C.; Scandolo, S.; Sclauzero, G.;

- Seitsonen, A. P.; Smogunov, A.; Umari, P.; Wentzcovitch, R. M., QUANTUM ESPRESSO: a modular and open-source software project for quantum simulations of materials. *J. Phys.: Condens. Matter* **2009**, *21* (39), 395502.
38. Perdew, J. P.; Burke, K.; Ernzerhof, M., Generalized Gradient Approximation Made Simple. *Phys. Rev. Lett.* **1996**, *77* (18), 3865-3868.
39. Troullier, N.; Martins, J. L., Efficient pseudopotentials for plane-wave calculations. *Phys. Rev. B* **1991**, *43* (3), 1993-2006.
40. Kleinman, L.; Bylander, D. M., Efficacious Form for Model Pseudopotentials. *Phys. Rev. Lett.* **1982**, *48* (20), 1425-1428.
41. Pickard, C. J.; Mauri, F., All-electron magnetic response with pseudopotentials: NMR chemical shifts. *Phys. Rev. B* **2001**, *63* (24), 245101.
42. Pyykkö, P., Year-2008 nuclear quadrupole moments. *Mol. Phys.* **2008**, *106* (16-18), 1965-1974.
43. Hafner, J., Ab-initio simulations of materials using VASP: Density-functional theory and beyond. *J. Comput. Chem.* **2008**, *29* (13), 2044-2078.
44. VandeVondele, J.; Krack, M.; Mohamed, F.; Parrinello, M.; Chassaing, T.; Hutter, J., Quickstep: Fast and accurate density functional calculations using a mixed Gaussian and plane waves approach. *Comput. Phys. Commun.* **2005**, *167* (2), 103-128.
45. Grimme, S.; Antony, J.; Ehrlich, S.; Krieg, H., A consistent and accurate ab initio parametrization of density functional dispersion correction (DFT-D) for the 94 elements H-Pu. *J. Chem. Phys.* **2010**, *132* (15), 154104.
46. Goedecker, S.; Teter, M.; Hutter, J., Separable dual-space Gaussian pseudopotentials. *Phys. Rev. B* **1996**, *54* (3), 1703-1710.
47. VandeVondele, J.; Hutter, J., Gaussian basis sets for accurate calculations on molecular systems in gas and condensed phases. *J. Chem. Phys.* **2007**, *127* (11), 114105.
48. Špačková, J.; Fabra, C.; Mittlelette, S.; Gaillard, E.; Chen, C.-H.; Cazals, G.; Lebrun, A.; Sene, S.; Berthomieu, D.; Chen, K.; Gan, Z.; Gervais, C.; Métro, T.-X.; Laurencin, D., Unveiling the Structure and Reactivity of Fatty-Acid Based (Nano)materials Thanks to Efficient and Scalable 17O and 18O-Isotopic Labeling Schemes. *J. Am. Chem. Soc.* **2020**, *142* (50), 21068-21081.
49. Dudognon, E.; Correia, N. T.; Danède, F.; Descamps, M., Solid-Solid Transformation in Racemic Ibuprofen. *Pharm. Res.* **2013**, *30* (1), 81-89.
50. Filsinger, B.; Zimmermann, H.; Haeberlen, U., 17O NMR evidence for 180°-flips of (COOH)₂ units in dimethylmalonic acid. *Mol. Phys.* **1992**, *76* (1), 157-172.
51. Carignani, E.; Borsacchi, S.; Geppi, M., Detailed Characterization of the Dynamics of Ibuprofen in the Solid State by a Multi-Technique NMR Approach. *ChemPhysChem* **2011**, *12* (5), 974-981.
52. Demkin, A. G.; Kolesov, B. A., Tautomeric Hydrogen Bond in Dimers of Ibuprofen. *J. Phys. Chem. A* **2019**, *123* (26), 5537-5541.
53. Ostrowska, K.; Kropidłowska, M.; Katrusiak, A., High-Pressure Crystallization and Structural Transformations in Compressed R,S-Ibuprofen. *Cryst. Growth Des.* **2015**, *15* (3), 1512-1517.
54. A similar energy difference was calculated when changing the initial OH positions before geometry relaxation, starting from different .cif files (corresponding to neutron or X-ray structures), and modifying the dispersion energy parameters in VASP.
55. Idziak, S., N.M.R. study of the molecular dynamics in crystalline trichloroacetic acid. *Mol. Phys.* **1989**, *68* (6), 1335-1340.
56. Carignani, E.; Borsacchi, S.; Marini, A.; Mennucci, B.; Geppi, M., 13C Chemical Shielding Tensors: A Combined Solid-State NMR and DFT Study of the Role of Small-Amplitude Motions. *J. Phys. Chem. C* **2011**, *115* (50), 25023-25029.
57. Geppi, M.; Guccione, S.; Mollica, G.; Pignatello, R.; Veracini, C. A., Molecular Properties of Ibuprofen and Its Solid Dispersions with Eudragit RL100 Studied by Solid-State Nuclear Magnetic Resonance. *Pharm. Res.* **2005**, *22* (9), 1544-1555.
58. Kolesov, B. A., Proton delocalization and tunneling in terephthalic acid: Raman spectroscopic study. *J. Phys. Chem. Solids* **2020**, *138*, 109288.

59. Goossens, D. J.; Chan, E. J., Synchrotron X-ray diffuse scattering from a stable polymorphic material: terephthalic acid, C₈H₆O₄. *Acta Crystallogr. Sect. B* **2017**, *73* (1), 112-121.
60. Beckham, G. T.; Peters, B.; Starbuck, C.; Variankaval, N.; Trout, B. L., Surface-Mediated Nucleation in the Solid-State Polymorph Transformation of Terephthalic Acid. *J. Am. Chem. Soc.* **2007**, *129* (15), 4714-4723.
61. Śledź, M.; Janczak, J.; Kubiak, R., New crystalline modification of terephthalic acid. *J. Mol. Struct.* **2001**, *595* (1), 77-82.
62. Davey, R. J.; Maginn, S. J.; Andrews, S. J.; Black, S. N.; Buckley, A. M.; Cottier, D.; Dempsey, P.; Plowman, R.; Rout, J. E.; Stanley, D. R.; Taylor, A., Morphology and polymorphism in molecular crystals: terephthalic acid. *J. Chem. Soc., Faraday Trans.* **1994**, *90* (7), 1003-1009.
63. Meier, B. H.; Ernst, R. R., Structure and dynamics of terephthalic acid from 2 to 300 K: II. The temperature dependence of the disorder: A solid-state NMR study. *J. Solid State Chem.* **1986**, *61* (1), 126-129.
64. Bailey, M.; Brown, C. J., The crystal structure of terephthalic acid. *Acta Crystallogr.* **1967**, *22* (3), 387-391.
65. Pritchina, E. A.; Kolesov, B. A., Raman spectra of terephthalic acid crystals in the temperature range 5K–300K. *Spectroc. Acta A* **2018**, *202*, 319-323.
66. McKinnon, J. J.; Fabbiani, F. P. A.; Spackman, M. A., Comparison of Polymorphic Molecular Crystal Structures through Hirshfeld Surface Analysis. *Cryst. Growth Des.* **2007**, *7* (4), 755-769.
67. Bauer, S.; Storek, M.; Gainaru, C.; Zimmermann, H.; Böhmer, R., Molecular Motions in Supercooled and Glassy Ibuprofen: Deuteron Magnetic Resonance and High-Resolution Rheology Study. *J. Phys. Chem. B* **2015**, *119* (15), 5087-5095.
68. Poplett, I. J. F.; Smith, J. A. S., ¹⁷O and ²H quadrupole double resonance in some carboxylic acid dimers. *J. Chem. Soc., Faraday Trans. 2* **1981**, *77* (8), 1473-1485.
69. Dudognon, E.; Danède, F.; Descamps, M.; Correia, N. T., Evidence for a New Crystalline Phase of Racemic Ibuprofen. *Pharm. Res.* **2008**, *25* (12), 2853-2858.
70. Adrjanowicz, K.; Kaminski, K.; Dulski, M.; Włodarczyk, P.; Bartkowiak, G.; Popena, L.; Jurga, S.; Kujawski, J.; Kruk, J.; Bernard, M. K.; Paluch, M., Communication: Synperiplanar to antiperiplanar conformation changes as underlying the mechanism of Debye process in supercooled ibuprofen. *J. Chem. Phys.* **2013**, *139* (11), 111103.
71. Tielens, F.; Folliet, N.; Bondaz, L.; Etemovic, S.; Babonneau, F.; Gervais, C.; Azaïs, T., Molecular Picture of the Adsorption of Ibuprofen and Benzoic Acid on Hydrated Amorphous Silica through DFT-D Calculations Combined with Solid-State NMR Experiments. *J. Phys. Chem. C* **2017**, *121* (32), 17339-17347.
72. Pourpoint, F.; Trébosc, J.; Gauvin, R. M.; Wang, Q.; Lafon, O.; Deng, F.; Amoureux, J.-P., Measurement of Aluminum–Carbon Distances Using S-RESPDOR NMR Experiments. *ChemPhysChem* **2012**, *13* (16), 3605-3615.
73. van Wüllen, L.; Koller, H.; Kalwei, M., Modern solid state double resonance NMR strategies for the structural characterization of adsorbate complexes involved in the MTG process. *Phys. Chem. Chem. Phys.* **2002**, *4* (9), 1665-1674.
74. Makrinich, M.; Sambol, M.; Goldbourn, A., Distance measurements between carbon and bromine using a split-pulse PM-RESPDOR solid-state NMR experiment. *Phys. Chem. Chem. Phys.* **2020**, *22*, 21022-21030.